Eur. Phys. J. C 29, 265–270 (2003)
Digital Object Identifier (DOI) 10.1140/epjc/s2003-01227-0

THE EUROPEAN PHYSICAL JOURNAL C

Fourth generation effects in processes induced by the $b \to s$ transition

T.M. Aliev[1,a], A. Özpineci[2,b], M. Savcı[1,c]

[1] Physics Department, Middle East Technical University, 06531 Ankara, Turkey
[2] The Abdus Salam International Center for Theoretical Physics, 34100, Trieste, Italy

Received: 3 April 2003 /
Published online: 2 June 2003 –

Abstract. We study the effects of sequential fourth quark generation in rare $B \to K(K^*)\ell^+\ell^-$ decays induced by the $b \to s$ transition and in B_s^0–$\bar{B}_s^0$ mixing. Using the experimental values on the branching ratios of the $B \to X_s\gamma$ and $B \to K(K^*)\ell^+\ell^-$ decays, the allowed regions for $|V_{tb}V_{ts}^*|$ and $|V_{t'b}V_{t's}^*|$ are determined as a function of the t' quark mass.

1 Introduction

Despite the fact that the standard model (SM) successfully describes all low energy experiments, it is an incomplete theory. This theory contains many unsolved and fundamental problems, such as the origin of CP violation, the mass spectrum and the number of generations. The recent observation of neutrino oscillations [1] indicated that the neutrino sector of SM must be enlarged. One of the most straightforward and economical extensions of the SM is to add a fourth generation to the fermionic sector, similar to the three-generation case. The extra generation can contribute to the electroweak radiative corrections. The latest studies in the electroweak sector allow for the existence of a fourth generation with a heavy Dirac neutrino [2,3]. Moreover, two or three extra generations with relatively "light" neutrinos, with a mass about 50 GeV are also allowed [3]. Flavor-changing neutral current (FCNC) transitions potentially provide the most sensitive and stringent test for the SM at loop level, since they are forbidden in the SM at tree level. At the same time these transitions are very sensitive to new physics beyond the SM via contributions of the new particles to the loop diagrams. It should be stressed that if newly proposed particles are heavy and if they cannot be produced directly in the accelerators, their influence through the loop diagrams can be a unique possibility for establishing new physics beyond the SM. The effects of the fourth generation to rare decays have been studied in many works [4–8].

Although theoretically FCNC processes are highly suppressed in the SM, very exciting results are obtained on the experimental side. The first measurements of the FCNC processes through $b \to s\gamma$ were reported by CLEO [9]. Recently, $B \to K\ell^+\ell^-$ decay has been observed at the B factories at SLAC and KEK [10–12]. The BaBar Collaboration also reported its preliminary results about the observation of $B \to K^*\ell^+\ell^-$ decay with branching ratio $\mathcal{B}(B \to K^*\ell^+\ell^-) = \left(1.68^{+0.68}_{-0.58} \pm 0.28\right) \times 10^{-6}$ and 90% C.L. $\mathcal{B}(B \to K^*\ell^+\ell^-) < 3 \times 10^{-6}$ [12]. In this paper, we study the contributions of the fourth generation to the processes induced by the $b \to s$ transitions and use the experimental results of the branching ratio for the $b \to s\gamma$ [13], $B \to K\ell^+\ell^-$ and $B \to K^*\ell^+\ell^-$ decays and try to determine the constraints on the extended Cabibbo–Kobayashi–Maskawa matrix (CKM) elements $|V_{tb}V_{ts}^*|$ and $|V_{t'b}V_{t's}^*|$.

This paper is organized as follows. In Sect. 2, we present the basic theoretical expressions for the differential widths of the $B \to K\ell^+\ell^-$ and $B \to K^*\ell^+\ell^-$ decays, and for the mass difference Δm_{B_s}, with sequential up-like quark in the fourth generation model. Section 3 is devoted to a numerical analysis and the conclusions.

2 Theoretical results

In this section we present the necessary theoretical formulae for the $B \to X_s\gamma$, $B \to K\ell^+\ell^-$, $B \to K^*\ell^+\ell^-$ decays and for the mass difference in the B_s^0–$\bar{B}_s^0$ system in the presence of the fourth generation. All these processes, except mixing in the B_s^0–$\bar{B}_s^0$ system, are induced by the $b \to s$ transition. At the quark level this transition is described by the effective Hamiltonian

$$\mathcal{H}_{\rm eff} = \frac{\alpha G_{\rm F}}{2\sqrt{2}\pi} V_{tb}V_{ts}^* \sum_{i=1}^{10} C_i(\mu)\mathcal{O}_i(\mu), \qquad (1)$$

where the full set of operators in $\mathcal{O}_i(\mu)$ and the corresponding expressions for the Wilson coefficients in the

[a] e-mail: taliev@metu.edu.tr
[b] e-mail: ozpineci@ictp.trieste.it
[c] e-mail: savci@metu.edu.tr

SM3 (here and in all further discussions SM3 and SM4 will denote SM with three and four generations, respectively) are given in [14,15]. As is well known, the fourth generation introduces the first three generations into SM copiously, and hence it is clear that it changes only the values of the Wilson coefficients $C_7(\mu)$, $C_9(\mu)$ and $C_{10}(\mu)$ with the help of the running fourth generation up quark t' at loop level and does not introduce any new operator structure, i.e.,

$$
\begin{aligned}
C_7^{\rm tot}(\mu) &= C_7^{\rm SM}(\mu) + \frac{V_{t'b}V_{t's}^*}{V_{tb}V_{ts}^*}C_7^{t'}(\mu),\\
C_9^{\rm tot}(\mu) &= C_9^{\rm SM}(\mu) + \frac{V_{t'b}V_{t's}^*}{V_{tb}V_{ts}^*}C_9^{t'}(\mu),\\
C_{10}^{\rm tot}(\mu) &= C_{10}^{\rm SM}(\mu) + \frac{V_{t'b}V_{t's}^*}{V_{tb}V_{ts}^*}C_{10}^{t'}(\mu),
\end{aligned}
\tag{2}
$$

where $V_{t'b}$ and $V_{t's}$ are the elements of the 4×4 Cabibbo–Kobayashi–Maskawa (CKM) matrix. The explicit forms of the $C_i^{t'}$ can easily be obtained from the SM results by simply substituting $m_t \to m_{t'}$. Neglecting the s quark mass, the effective Hamiltonian leads to the following matrix element for the $b \to s\ell^+\ell^-$ transition:

$$
\begin{aligned}
\mathcal{M} = {} & \frac{G\alpha}{2\sqrt{2}\pi}V_{tb}V_{ts}^*\\
& \times \Big[C_9^{\rm tot}\,\bar{s}\gamma_\mu(1-\gamma_5)b\,\bar{\ell}\gamma_\mu\ell + C_{10}^{\rm tot}\,\bar{s}\gamma_\mu(1-\gamma_5)b\,\bar{\ell}\gamma_\mu\gamma_5\ell\\
& - 2C_7^{\rm tot}\frac{m_b}{q^2}\bar{s}\sigma_{\mu\nu}q^\nu(1+\gamma_5)b\,\bar{\ell}\gamma_\mu\ell\Big],
\end{aligned}
\tag{3}
$$

where $q^2 = (p_1+p_2)^2$ and p_1 and p_2 are the four-momenta of the final leptons. We observe from (3) that in order to calculate the matrix element for the $B \to K^*(K)\ell^+\ell^-$ decay, the matrix elements of the quark operators in (3) need to be sandwiched between initial and final (K or K^*) meson states, which results in a form that is parametrized in terms of the form factors:

$$
\begin{aligned}
&\langle K^*(p_{K^*},\varepsilon)\,|\bar{s}\gamma_\mu(1-\gamma_5)b|\,B(p_B)\rangle\\
&= -{\rm i}\varepsilon_\mu^*(m_B+m_{K^*})A_1(q^2)\\
&\quad +{\rm i}(p_B+p_{K^*})_\mu(\varepsilon^*q)\frac{A_2(q^2)}{m_B+m_{K^*}}\\
&\quad +{\rm i}q_\mu\frac{2m_{K^*}}{q^2}(\varepsilon^*q)\left[A_3(q^2)-A_0(q^2)\right]\\
&\quad -\epsilon_{\mu\nu\lambda\sigma}\varepsilon^{*\nu}p_{K^*}^\lambda q^\sigma\frac{2V(q^2)}{m_B+m_{K^*}},
\end{aligned}
\tag{4}
$$

where ε is the polarization vector of K^* meson and $q = p_B - p_{K^*}$ is the momentum transfer. Using the equation of motion, the form factor $A_3(q^2)$ can be written in terms of $A_1(q^2)$ and $A_2(q^2)$ as follows:

$$
A_3(q^2) = \frac{(m_B+m_{K^*})}{2m_{K^*}}A_1(q^2) - \frac{(m_B-m_{K^*})}{2m_{K^*}}A_2(q^2). \tag{5}
$$

In order to ensure that there exists no kinematical singularity we assume that $A_3(q^2=0) = A_0(q^2=0)$.

The corresponding form factors are defined through the matrix elements for the $B \to K$ transition by

$$
\begin{aligned}
&\langle K(p_K)\,|\bar{s}\gamma_\mu b|\,B(p_B)\rangle\\
&= f_+\left[(p_B+p_K)_\mu - \frac{m_B^2-m_K^2}{q^2}\,q_\mu\right] + f_0\,\frac{m_B^2-m_K^2}{q^2}\,q_\mu.
\end{aligned}
\tag{6}
$$

The finiteness of (6) is guaranteed by demanding $f_+(0) = f_0(0)$.

The semileptonic form factors for the K^* and K mesons resulting from the dipole operator $\bar{s}{\rm i}\sigma_{\mu\nu}q^\nu(1+\gamma_5)b$ are defined by

$$
\begin{aligned}
&\langle K^*(p_{K^*},\varepsilon)\,|\bar{s}{\rm i}\sigma_{\mu\nu}q^\nu(1+\gamma_5)b|\,B(p_B)\rangle\\
&= 2\epsilon_{\mu\nu\lambda\sigma}\varepsilon^{*\nu}p_{K^*}^\lambda q^\sigma T_1(q^2)\\
&\quad +{\rm i}\left[\varepsilon_\mu^*(m_B^2-m_{K^*}^2) - (p_B+p_{K^*})_\mu(\varepsilon^*q)\right]T_2(q^2)\\
&\quad +{\rm i}(\varepsilon^*q)\left[q_\mu - (p_B+p_{K^*})_\mu\frac{q^2}{m_B^2-m_{K^*}^2}\right]T_3(q^2),
\end{aligned}
\tag{7}
$$

$$
\begin{aligned}
&\langle K(p_K)\,|\bar{s}{\rm i}\sigma_{\mu\nu}q^\nu(1+\gamma_5)b|\,B(p_B)\rangle\\
&= -\frac{f_T}{m_B+m_K}[(p_B+p_K)_\mu q^2 - q_\mu(m_B^2-m_K^2)].
\end{aligned}
\tag{8}
$$

The matrix elements of the $B \to K\ell^+\ell^-$ and $B \to K^*\ell^+\ell^-$ decays can be written

$$
\mathcal{M} = \frac{G\alpha}{2\sqrt{2}\pi}V_{tb}V_{ts}^*m_B\left(F_\mu^{1i}\bar{\ell}\gamma_\mu\ell + F_\mu^{2i}\bar{\ell}\gamma_\mu\gamma_5\ell\right), \tag{9}
$$

where $i=1$ corresponds to the K meson and $i=2$ corresponds to the K^* meson, respectively, and

$$
F_\mu^{11} = \frac{1}{m_B}\left[A'(p_B+p_K)_\mu + B'q_\mu\right], \tag{10}
$$

$$
F_\mu^{21} = \frac{1}{m_B}\left[C'(p_B+p_K)_\mu + D'q_\mu\right], \tag{11}
$$

$$
\begin{aligned}
F_\mu^{12} = {} & \Bigg[-\frac{1}{m_B^2}A\epsilon_{\mu\nu\rho\sigma}\varepsilon^{*\nu}p_{K^*}^\rho q^\sigma - {\rm i}B_1\varepsilon_\mu^*\\
& +{\rm i}\frac{1}{m_B^2}B_2(\varepsilon^*q)p_{K^*\mu} + {\rm i}\frac{1}{m_B^2}B_3(\varepsilon^*q)q_\mu\Bigg],
\end{aligned}
\tag{12}
$$

$$
\begin{aligned}
F_\mu^{22} = {} & \Bigg[-\frac{1}{m_B^2}C_1\epsilon_{\mu\nu\rho\sigma}\varepsilon^{*\nu}p_{K^*}^\rho q^\sigma - {\rm i}D_1\varepsilon_\mu^*\\
& +{\rm i}\frac{1}{m_B^2}D_2(\varepsilon^*q)p_{K^*\mu} + {\rm i}\frac{1}{m_B^2}D_3(\varepsilon^*q)q_\mu\Bigg],
\end{aligned}
\tag{13}
$$

where

$$
\begin{aligned}
A' &= C_9^{\rm tot}f_+ + 2\frac{m_b}{m_B}\frac{1}{(1+\sqrt{r})}C_7^{\rm tot}f_T,\\
B' &= C_9^{\rm tot}f_+ + 2\frac{m_b}{m_B}\frac{(1-\sqrt{r})}{s}C_7^{\rm tot}f_T,\\
C' &= C_{10}^{\rm tot}f_+,\\
D' &= C_{10}^{\rm tot}f_-,\\
A &= \frac{2V}{1+\sqrt{r}}C_9^{\rm tot} + 4\frac{m_b}{m_Bs}C_7^{\rm tot}T_1,
\end{aligned}
$$

$$
\begin{aligned}
B_1 &= (1+\sqrt{r})\left[C_9^{\rm tot}A_1 + 2\frac{m_b}{m_B s}(1-\sqrt{r})C_7^{\rm tot}T_2\right],\\
B_2 &= \frac{1}{1-r}\left[(1-\sqrt{r})C_9^{\rm tot}A_2\right.\\
&\qquad \left. +2\frac{m_b}{m_B}C_7^{\rm tot}\left(T_3+\frac{1-r}{s}T_2\right)\right],\\
B_3 &= \frac{1}{s}\left[2\sqrt{r}C_9^{\rm eff}(A_3-A_0) - 2\frac{m_b}{m_B}C_7^{\rm tot}T_3\right],\\
C_1 &= \frac{2V}{1+\sqrt{r}}C_{10}^{\rm tot},\\
D_1 &= (1+\sqrt{r})C_{10}^{\rm tot}A_1,\\
D_2 &= \frac{A_2}{1+\sqrt{r}}C_{10}^{\rm tot},\\
D_3 &= \frac{2\sqrt{r}}{s}(A_3-A_0)C_{10}^{\rm tot},
\end{aligned}
\tag{14}
$$

where

$$
f_-(q^2) = \frac{(1-r)}{s}[f_0(q^2)-f_+(q^2)],\ r=\frac{m_{K^*}^2}{m_B^2},\quad s=\frac{q^2}{m_B^2}.
$$

Using the matrix element, for the dilepton invariant mass distribution we get

$$
\begin{aligned}
\frac{{\rm d}\Gamma^{B\to K}}{{\rm d}s} &= \frac{G^2\alpha^2 m_B^5}{2^{10}\pi^5}\left|V_{tb}V_{ts}^*\right|^2\sqrt{\lambda}\,v\\
&\times\left\{\frac{\lambda}{3}(3-v^2)\left(|A'|^2+|C'|^2\right)\right.\\
&\quad +s(1-v^2)(2+2r-s)\,|C'|^2\\
&\quad +2s(1-v^2)(1-r){\rm Re}\left[C'D'^*\right]\\
&\quad \left.+s^2(1-v^2)\,|D'|^2\right\},
\end{aligned}
\tag{15}
$$

$$
\begin{aligned}
\frac{{\rm d}\Gamma^{B\to K^*}}{{\rm d}s} &= \frac{G^2\alpha^2 m_B^5}{2^{10}\pi^5}\left|V_{tb}V_{ts}^*\right|^2\sqrt{\lambda}\,v\\
&\times\left\{\frac{1}{6}s\lambda\left(3-v^2\right)|A|^2+\frac{1}{3}s\lambda v^2\,|C_1|^2\right.\\
&\quad +\frac{1}{12r}\left[\left(3-v^2\right)(\lambda+12rs)\,|B_1|^2\right.\\
&\quad \left.+\left(\lambda\left(3-v^2\right)+24rsv^2\right)|D_1|^2\right]\\
&\quad +\frac{\lambda}{12r}\left[\lambda(3-v^2)\,|B_2|^2\right.\\
&\quad \left.+\left\{\lambda\left(3-v^2\right)+3\left(1-v^2\right)s(2+2r-s)\right\}|D_2|^2\right)\\
&\quad -\frac{\lambda}{6r}\left[\left(3-v^2\right)(1-r-s){\rm Re}\left[B_1B_2^*\right]\right.\\
&\quad \left.+\left\{\left(3-v^2\right)(1-r-s)+3\left(1-v^2\right)s\right\}{\rm Re}\left[D_1D_2^*\right]\right]\\
&\quad -\frac{\lambda}{2r}\left(1-v^2\right)s\left({\rm Re}\left[D_1D_3^*\right]-(1-r){\rm Re}\left[D_2D_3^*\right]\right)\\
&\quad \left.+\frac{\lambda}{4r}\left(1-v^2\right)s^2\,|D_3|^2\right\},
\end{aligned}
\tag{16}
$$

where $v^2=1-4m_\ell^2/q^2$ and $\lambda(a,b,c)=a^2+b^2+c^2-2ab-2ac-2bc$ is the usual triangle function.

In constraining up quark type fourth generation effects, we will also consider B_s^0–$\bar{B}_s^0$ mixing. The mass difference Δm_{B_s} in SM4 can be written as

$$
\begin{aligned}
\Delta m_{B_s} &= \frac{G^2m_W^2}{6\pi^2}m_{B_s}B_{B_s}f_{B_s}^2\\
&\times\left\{\eta_t\left(V_{tb}V_{ts}^*\right)^2S_0(x_t)+\eta_{t'}\left(V_{t'b}V_{t's}^*\right)^2S_0(x_{t'})\right.\\
&\quad \left.+2\eta_{tt'}\left(V_{tb}V_{ts}^*\right)\left(V_{t'b}V_{t's}^*\right)S(x_t,x_{t'})\right\},
\end{aligned}
\tag{17}
$$

where $x_t=m_t^2/m_W^2$, $x_{t'}=m_{t'}^2/m_W^2$ and

$$
S_0(x_t) = \frac{4x_t-11x_t^2+x_t^3}{4(1-x_t)^2}-\frac{3}{2}\frac{x_t^3\ln x_t}{(1-x_t)^3},
\tag{18}
$$

$$
S_0(x_{t'}) = S_0(x_t\to x_{t'}),
\tag{19}
$$

$$
\begin{aligned}
&S(x_t,x_{t'})\\
&= x_tx_{t'}\left\{\frac{1}{x_{t'}-x_t}\left[\frac{1}{4}+\frac{3}{2}\frac{1}{1-x_{t'}}-\frac{3}{4}\frac{1}{(1-x_{t'})^2}\right]\ln x_{t'}\right.\\
&\quad -\frac{1}{x_{t'}-x_t}\left[\frac{1}{4}+\frac{3}{2}\frac{1}{1-x_t}-\frac{3}{4}\frac{1}{(1-x_t)^2}\right]\ln x_t\\
&\quad \left.-\frac{3}{4}\frac{1}{(1-x_t)(1-x_{t'})}\right\}.
\end{aligned}
\tag{20}
$$

Here $\eta_t=0.55$ is the QCD correction factor. Taking into account the threshold effect from b' quark, $\eta_{tt'}$ is estimated to be [7]

$$
\eta_{tt'} = (\alpha_s(m_t))^{6/23}\left(\frac{\alpha_s(m_{b'})}{\alpha_s(m_t)}\right)^{6/21}\left(\frac{\alpha_s(m_{t'})}{\alpha_s(m_{b'})}\right)^{6/19}.
$$

Note that when $m_{t'}$ lies between 250 GeV and 400 GeV, $\eta_{tt'}$ is quite close to $\eta_{t'}$ numerically; hence, for simplicity, in our further analysis we will set $\eta_{tt'}=\eta_{t'}$.

In order to obtain quantitative results the value of the fourth generation CKM matrix element $V_{t'b}V_{t's}^*$ is needed. To this aim we will use the experimentally measured values of the branching ratios $\mathcal{B}(B\to X_s\gamma)$ and $\mathcal{B}(B\to X_ce\bar{\nu}_e)$. To eliminate the uncertainty coming from the b quark mass we consider the ratio

$$
R = \frac{\mathcal{B}(B\to X_s\gamma)}{\mathcal{B}(B\to X_ce\bar{\nu}_e)}.
\tag{21}
$$

In leading logarithmic approximation this ratio is equal to

$$
R = \frac{6\alpha\left|C_7^{\rm tot}(m_b)V_{tb}V_{ts}^*\right|^2}{\pi f(\hat{m}_c)\kappa(\hat{m}_c)\left|V_{cb}\right|^2},
\tag{22}
$$

where $\hat{m}_c=m_c/m_b$ and the functions $f(\hat{m}_c)$ and $\kappa(\hat{m}_c)$ for the $b\to c\ell\bar{\nu}$ transition are given by [16]

$$
\begin{aligned}
f(\hat{m}_c) &= 1-8\hat{m}_c^2+8\hat{m}_c^6-\hat{m}_c^8-24\hat{m}_c^4\ln(\hat{m}_c),\\
\kappa(\hat{m}_c) &= 1-\frac{2\alpha_s(m_b)}{3\pi}\left[\left(\pi^2-\frac{31}{4}\right)\left(1-\hat{m}_c^2\right)^2+\frac{3}{2}\right].
\end{aligned}
\tag{23}
$$

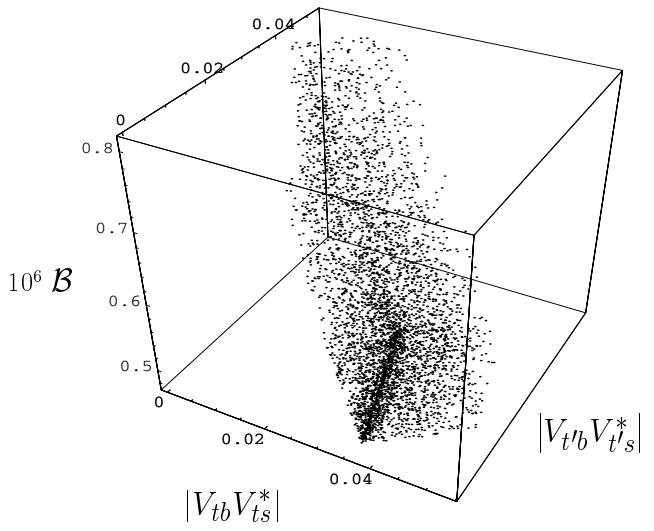

Fig. 1. Three-dimensional plot of the branching ratio for the $B \to K\ell^+\ell^-$ decay, with respect to the allowed parameter space of $V_{tb}V_{ts}^*$ and $V_{t'b}V_{t's}^*$, at $m_{t'} = 200\,\mathrm{GeV}$

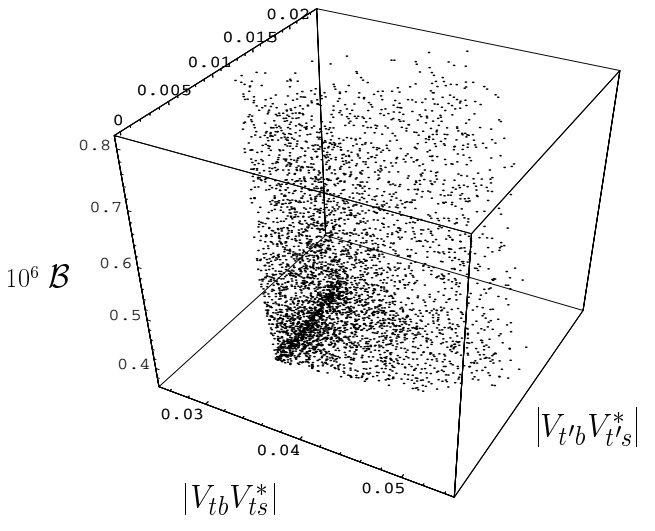

Fig. 2. The same as in Fig. 1, but at $m_{t'} = 300\,\mathrm{GeV}$

Table 1. B meson decay form factors in a three-parameter fit, where the radiative corrections to the leading twist contribution and SU(3) breaking effects are taken into account [22,23]

	$F(0)$	a_F	b_F
$f_+^{B\to K}$	0.35	1.37	0.35
$f_0^{B\to K}$	0.35	0.40	0.41
$A_1^{B\to K^*}$	0.337	0.60	−0.023
$A_2^{B\to K^*}$	0.283	1.18	0.281
$A_0^{B\to K^*}$	0.470	1.55	0.68
$V^{B\to K^*}$	0.458	1.55	0.575
$T_1^{B\to K^*}$	0.379	1.59	0.615
$T_2^{B\to K^*}$	0.379	0.49	−0.241
$T_3^{B\to K^*}$	0.261	1.20	0.098

From (21) and (22) we get

$$\left|C_7^{\mathrm{SM}}V_{tb}V_{ts}^* + C_7^{\mathrm{new}}V_{t'b}V_{t's}^*\right| = \sqrt{\frac{\pi f(\hat{m}_c)\kappa(\hat{m}_c)\left|V_{cb}\right|^2}{6\alpha}\,\frac{\mathcal{B}(B\to X_s\gamma)}{\mathcal{B}(B\to X_ce\bar{\nu}_e)}}. \quad (24)$$

The model parameters can be constrained from the measured branching ratios of the $B \to X_s\gamma$ decay and $\mathcal{B}(B \to X_ce\bar{\nu}_e) = 10.4\%$:

$$\mathcal{B}(B\to X_s\gamma) = \begin{cases} \left(3.21 \pm 0.43 \pm 0.27^{+0.18}_{-0.10}\right)\times 10^{-4} & [17], \\ (3.36 \pm 0.53 \pm 0.42 \pm 0.54)\times 10^{-4} & [18], \\ (3.11 \pm 0.80 \pm 0.72)\times 10^{-4} & [19]. \end{cases}$$

In our numerical analysis, we will use the weighted average value $\mathcal{B}(B \to X_s\gamma) = (3.23 \pm 0.42)\times 10^{-4}$ [20] for the branching ratio of the $B \to X_s\gamma$ decay.

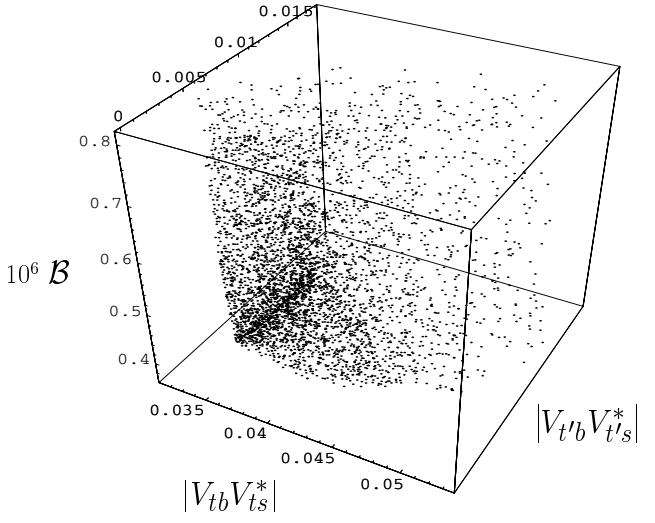

Fig. 3. The same as in Fig. 1, but at $m_{t'} = 400\,\mathrm{GeV}$

Another constraint to the extended CKM matrix element comes from the unitarity condition, i.e.,

$$\begin{aligned} &|V_{us}|^2 + |V_{cs}|^2 + |V_{ts}|^2 + |V_{t's}|^2 = 1, \\ &|V_{ub}|^2 + |V_{cb}|^2 + |V_{tb}|^2 + |V_{t'b}|^2 = 1, \\ &V_{ub}V_{us}^* + V_{cb}V_{cs}^* + V_{tb}V_{ts}^* + V_{t'b}V_{t's}^* = 0. \end{aligned} \quad (25)$$

Since charged-current tree-level decays are well measured experimentally they are not affected by new physics at leading order. Therefore, for the parameters $|V_{us}|$, $|V_{cs}|$, $|V_{cb}|$ and $|V_{ub}/V_{cb}|$ we will make use of the Particle Data Group (PDG) constraints [13]. Using the weighted average for $\mathcal{B}(B \to X_s\gamma)$ and the PDG constraint $0.38 \le |V_{cb}| \le 0.044$, from (24) and (25) we get the constraints

$$0.011 \le \left|C_7^{\mathrm{SM}}V_{tb}V_{ts}^* + C_7^{\mathrm{new}}V_{t'b}V_{t's}^*\right| \le 0.015, \quad (26)$$

$$0.03753 \le |V_{tb}V_{ts}^* + V_{t'b}V_{t's}^*| \le 0.043976, \quad (27)$$

$$0 \le |V_{ts}|^2 + |V_{t's}|^2 \le 0.00492, \quad (28)$$

$$0.998 \le |V_{tb}|^2 + |V_{t'b}|^2 \le 0.9985. \quad (29)$$

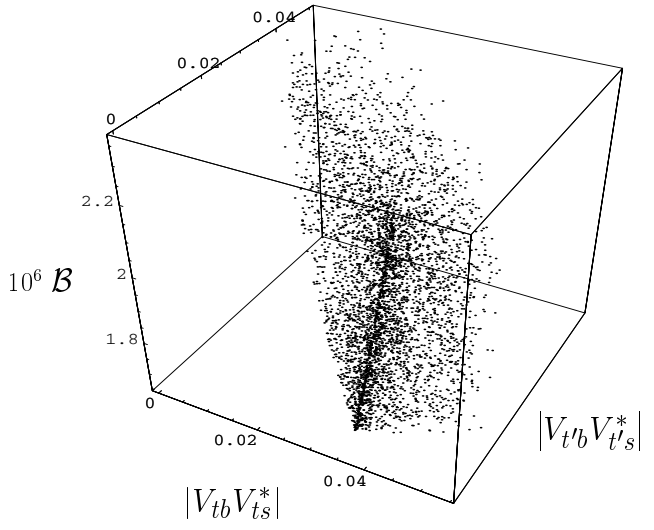

Fig. 4. The same as in Fig. 1, but for the $B \to K^*\ell^+\ell^-$ decay

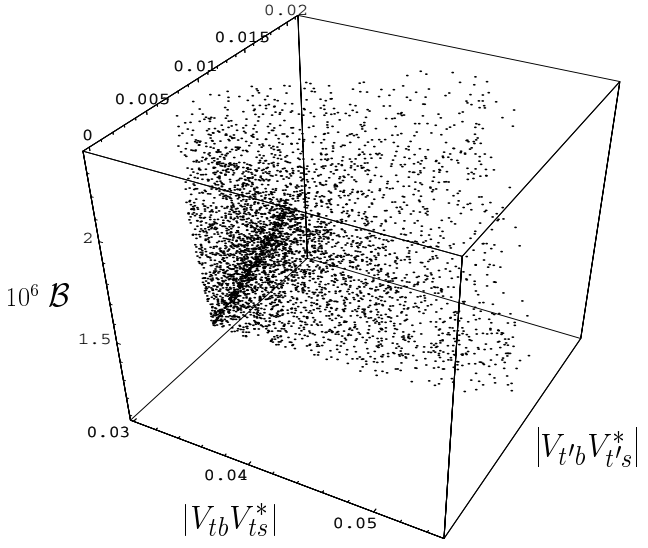

Fig. 5. The same as in Fig. 4, but at $m_{t'} = 300\,\mathrm{GeV}$

3 Numerical analysis

In this section we will study the constraints to $|V_{t'b}V_{t's}^*|$ coming from the measured branching ratios of the $B \to K\ell^+\ell^-$ and $B \to K^*\ell^+\ell^-$ decays and B_s^0–$\bar{B}_s^0$ mixing, as well as using the results in (26)–(29). The main input parameters involved in a calculation of the branching ratios of the $B \to K\ell^+\ell^-$ and $B \to K^*\ell^+\ell^-$ decays are the form factors, whose values we take from the light cone QCD sum rule [21–23], where the form factors are expressed in terms of three parameters as follows:

$$F(s) = \frac{F(0)}{1 - a_F s + b_F s^2},$$

where the values of parameters $F(0)$, a_F and b_F for the $B \to K$ and $B \to K^*$ decay are listed in Table 1.

The values of the other input parameters which we use in our numerical calculations are $m_b = 4.8\,\mathrm{GeV}$, $m_c = 1.35\,\mathrm{GeV}$, $m_{B_s} = 5.369\,\mathrm{GeV}$, $\tau_{B_s} = 1.64 \times 10^{-12}\,\mathrm{s}$ and $B_{B_s} f_{B_s}^2 = (0.26\,\mathrm{GeV})^2$. The experimental lower bound of the mass difference is $\Delta m_{B_s} \geq 14.9\,\mathrm{ps}^{-1}$. For the values of the Wilson coefficients C_7^{SM}, C_9^{SM} and C_{10}^{SM} we have used their next-to-leading logarithmic result: $C_7^{\mathrm{SM}} = -0.308$, $C_9^{\mathrm{SM}} = 4.154$ and $C_{10}^{\mathrm{SM}} = -4.261$. It should be noted that the decays $B \to K\ell^+\ell^-$ and $B \to K^*\ell^+\ell^-$ receive a long distance contribution coming from the $\bar{c}c$ intermediate states. In the present work we neglect such long distance effects. The strong dependence on $m_{t'}$ (see for example [4]) makes the electroweak penguins a good place to look for the existence of a fourth generation. Contributions of a fourth generation to $B \to K(K^*)\ell^+\ell^-$ decays have already been studied (see the second references in [4] and [6]). The present investigation differs from the abovementioned works in two aspects:

(1) we use the experimentally measured results on the branching ratio;

(2) we consider $V_{tb}V_{ts}^*$ and $V_{t'b}V_{t's}^*$ as two independent complex parameters; these were taken to be real in [4,6].

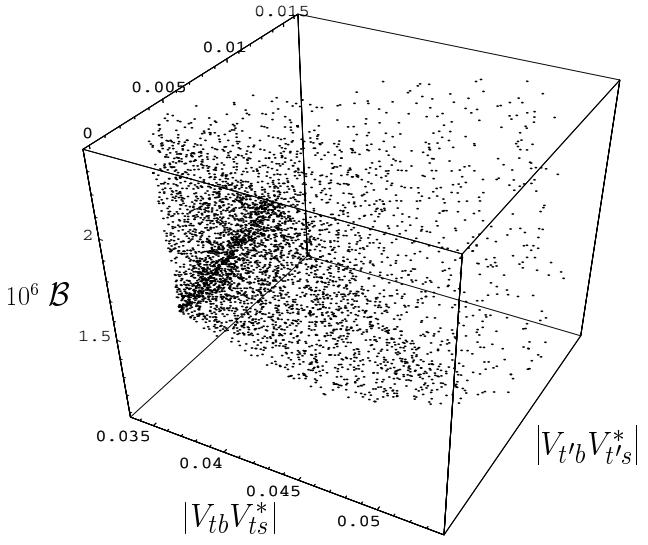

Fig. 6. The same as in Fig. 4, but at $m_{t'} = 400\,\mathrm{GeV}$

The complex parameters $V_{tb}V_{ts}^*$ and $V_{t'b}V_{t's}^*$ are constrained by the unitarity conditions (see (27)–(29)), the measured branching ratios $B \to X_s\gamma$ (see (26)) and $B \to K(K^*)\ell^+\ell^-$ decays (see (15) and (16)), which depend on $m_{t'}$. For each value of $m_{t'}$ there exists an allowed region in the $|V_{tb}V_{ts}^*|$–$|V_{t'b}V_{t's}^*|$ plane.

Since there exists no analytical solution of (26)–(29), we will solve these equations numerically assuming that $V_{tb}V_{ts}^*$ and $V_{t'b}V_{t's}^*$ are complex. For a sufficiently large number of randomly chosen complex parameters $V_{t'b}V_{t's}^*$ and $V_{tb}V_{ts}^*$, the selected values would range over the whole solution space. In Figs. 1–3 we present the allowed region for $V_{tb}V_{ts}^*$ and $V_{t'b}V_{t's}^*$ at $m_{t'} = 200\,\mathrm{GeV}$, $m_{t'} = 300\,\mathrm{GeV}$ and $m_{t'} = 400\,\mathrm{GeV}$, respectively. In obtaining this solution the region we have used is as in (26)–(29) and (15). From these figures we see that, for $|V_{t'b}V_{t's}^*| = 0$, $|V_{tb}V_{ts}^*|$ takes on values that are close to the SM prediction and are mainly distributed around ~ 0.04. Moreover, when $|V_{t'b}V_{t's}^*|$ increases, the allowed region of $|V_{tb}V_{ts}^*|$

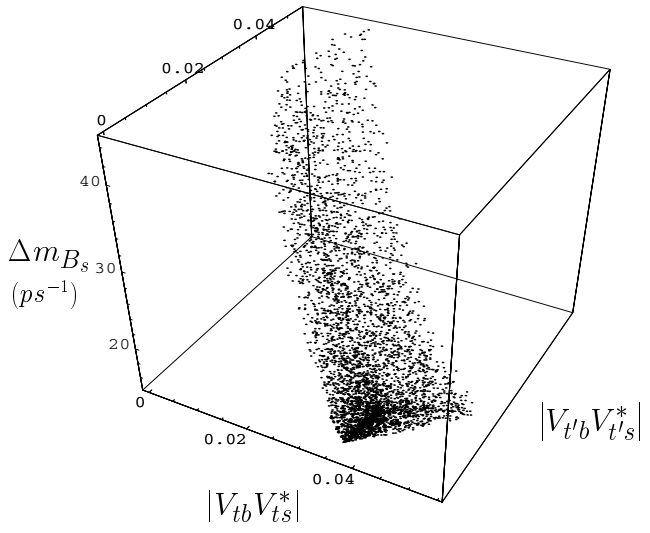

Fig. 7. Three-dimensional plot of the mass difference Δm_{B_s} of the B_s^0–$\bar{B}_s^0$ system, with respect to the allowed parameter space of $V_{tb}V_{ts}^*$ and $V_{t'b}V_{t's}^*$, at $m_{t'} = 300\,\mathrm{GeV}$

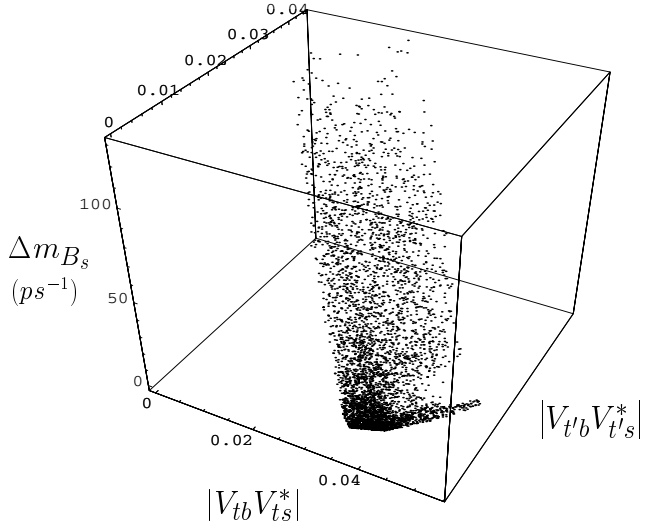

Fig. 8. The same as in Fig. 7, but at $m_{t'} = 700\,\mathrm{GeV}$

becomes wider with the center being fixed around 0.04, and the values of $|V_{t'b}V_{t's}^*|$ are mainly distributed around 0.01. With increasing values of $m_{t'}$, the allowed region for $|V_{t'b}V_{t's}^*|$ becomes narrower. This behavior can be explained as follows. The Wilson coefficients are strongly dependent on $m_{t'}$ and in order to remain in the experimentally allowed region, the element $|V_{t'b}V_{t's}^*|$ of the CKM matrix must decrease, since the branching ratio contains factors like $|C_i V_{tb}V_{ts}^*|$. A similar behavior is observed for the $B \to K^*\ell^+\ell^-$ decay (see Figs. 4–6).

In Figs. 7 and 8 we present the dependence of Δm_{B_s} on $|V_{tb}V_{ts}^*|$ and $|V_{t'b}V_{t's}^*|$, taking into account the lower experimental bound for Δm_{B_s}, at two different values of $m_{t'}$. It follows from both figures that the main distribution is in the range $0.36 \le |V_{tb}V_{ts}^*| \le 0.044$ and $0 \le |V_{t'b}V_{t's}^*| \le 0.01$. With increasing values of $m_{t'}$, obviously, Δm_{B_s} also increases.

Finally we would like to note that restrictions to the $|V_{t'd}V_{t'b}^*|$ matrix element can be obtained by an investigation of the rare decays induced through the $b \to d$ transition. A further analysis of the decays induced by the $b \to s(d)$ transition is more promising in studying new sources for CP violation, since the 4×4 CKM matrix predicts the existence of three CP violating phases. We will discuss this issue elsewhere in the future.

In conclusion, we have studied the effect of the fourth generation quark to the rare decays induced by the FCNC $b \to s$ transition. Using the experimental result for the branching ratios of the $B \to X_s\gamma$, $B \to K(K^*)\ell^+\ell^-$ decays and the unitarity condition for the 4×4 CKM matrix, we have determined the allowed parameter space for $|V_{tb}V_{ts}^*|$ and $|V_{t'b}V_{t's}^*|$ in their dependence on $m_{t'}$.

References

1. J.I. Silva-Marcos, JHEP **0212**, 036 (2002)
2. H.J. He, N. Polonsky, S. Su, Phys. Rev. D **64**, 053004 (2001)
3. V.A. Novikov, L.B. Okun, A.N. Rozanov, M.I. Vysotsky, Phys. Lett. B **529**, 111 (2002)
4. W.S. Hou, A. Soni, H. Steger, Phys. Lett. B **192**, 441 (1987); W.S. Hou, R.S. Willey, A. Soni, Phys. Rev. Lett. **58**, 1608 (1987); Erratum ibid. **60**, 2337 (1987)
5. A. Arhrib, W.S. Hou, Eur. Phys. J. C **27**, 555 (2003)
6. T.M. Aliev, D.A. Demir, N.K. Pak, Phys. Lett. B **389**, 83 (1996); T.M. Aliev, A. Özpineci, M. Savcı, Nucl. Phys. B **585**, 275 (2000); T.M. Aliev, A. Özpineci, M. Savcı, Eur. Phys. J. C **27**, 405 (2003)
7. T. Hattori, T. Hasuike, S. Wakaizumi, Phys. Rev. D **60**, 113008 (1999)
8. C.S. Huang, W.J. Huo, Y.L. Wu, Mod. Phys. Lett. A **14**, 2453 (1999); Phys. Rev. D **64**, 016009 (2001); W.J. Huo, Eur. J. Phys. C **24**, 275 (2002)
9. M.S. Alam et al., CLEO Collaboration, Phys. Rev. Lett. **74**, 2885 (1995)
10. K. Abe et al., Belle Collaboration, Phys. Rev. Lett. **88**, 021801 (2002)
11. B. Aubert et al., BaBar Collaboration, Phys. Rev. Lett. **88**, 241801 (2002)
12. B. Aubert et al., BaBar Collaboration, prep. hep-ex/0207082 (2002)
13. K. Hagiwara et al., Particle Data Group, Phys. Rev. D **66**, 010001 (2002)
14. G. Buchalla, A.J. Buras, Nucl. Phys. B **400**, 225 (1993)
15. M. Misiak, Nucl. Phys. B **398**, 23 (1993); Erratum ibid. B **439**, 461 (1995)
16. A.J. Buras, prep. hep-ph/9806471 (1998)
17. S. Chen et al., CLEO Collaboration, Phys. Rev. Lett. **87**, 251807 (2001)
18. H. Tajima, BELLE Collaboration, Int. J. Mod. Phys. A **17**, 2967 (2002)
19. R. Barate et al., ALEPH Collaboration, Phys. Lett. B **429**, 169 (1998)
20. P. Gambino, M. Misiak, Nucl. Phys. B **611**, 338 (2001)
21. T.M. Aliev, A. Özpineci, M. Savcı, Phys. Rev. D **55**, 7059 (1997)
22. P. Ball, V.M. Braun, Phys. Rev. D **58**, 094016 (1998)
23. P. Ball, prep. hep-ph/9803501 (1998)